JAST, Vol. 11, No. 1, pp. 21- 34

JAST
Journal of Aerospace Science and Technology

Local Imperfection Effects on Thermal Buckling Behavior of Composite Fiber Reinforced Truncated Conical Liner

S.A. Hosseini Kordkheili[1*], Z. Soltani[2] and A. Merati[3]

1, 2, 3. Center of Excellence in Aerospace Systems, Department of Aerospace Engineering, Sharif University of Technology,

*Azadi Avenue, Tehran, Iran

ali.hosseini@sharif.edu

Thermal buckling behavior of truncated conical liner reinforced by laminated composite is investigated in the presence of a general initial imperfection. For this purpose, the method of virtual work and first-order strain-deformation shell theory are employed to extract equilibrium equations. To this end, a finite element code is developed using the 3D 8-node shell element with six degrees of freedom as an analysis tool. Also, the variation of thickness in conical composite shell is considered. Several problems withc-c, s-s, c-f boundary conditions are solved using code to highlight the effect of imperfection size and position. In this way, the most effective imperfection at each boundary condition is determined.

Keywords: Thermal buckling, Composite shell, Finite element method, Local imperfection, Truncated conical liner

Introduction

The conical shells are used as transition parts between cylinders of different diameters and/or nozzles and sometimes as stand-alone components in various engineering applications such as tanks and pressure vessels. These structures often operate at elevated temperatures especially in gas turbine engines, satellites carrier rockets as well as missiles engines.

Advances in composite material technology causes daily increases in their applications in high temperature environments. Despite this achievement, employing composite made structures are still associated with some inherent difficulties mainly for mechanical connection with other part of structures. In order to deal with this problem, designers have proposed the usage of metal liner because of its more appropriate capability of making these connections as well as protecting the composite layers from direct exposure of heat.

In truncated conical liner with reinforced laminated composite shell structures, undesirable imperfection may take place in metal liner during the fabrication and/or carrying process.

An important concern for designing these kinds of structures is to estimate the change in critical buckling temperature as a result of the existence of imperfection.

Lissa [1], in his valuable study, has developed twelve different shell the oriesto analyze shell structures. Based on these theories, other researchers have struggled to solve their own problems using analytical or numerical methods. Panda and Natarajan [2] proposed a finite element formulation for composite shells with variable thickness for static analysis of composite plates and cylindrical shells. Cook [3] has provided a literature with composite shells buckling theory and finite element formulation together with the eigenvalue solution method.

1. Associate Professor (Corresponding Author)

Bathe [4] has also presented the finite element formulation for 8-noded degenerated shell element based on first-order shear deformation theory.

Based on different order shear deformation shell theories, thermal buckling of plates and/or conical shells made of FG materials have been in vestigated in Refs. [5, 6].

Considering uniform temperature rise, thermal buckling analysis of orthotropic cylindrical shells employing Rayleigh–Ritz method has been done without in corpora ting the pre-buckling rotations in [7] and with pre-buckling rotations in [8].

For the case of laminated composite cylindrical shells, the thermal buckling has been studied using finite element method for asymmetric circumferential nodes [9] and axi symmetric ones[10].

The influence of piezoelectric actuators [11] as well as internal hot fluid [12] on the thermal buckling characteristics of laminated cylindrical shells have been examined using semi-analytical finite element approach based on the first-order shear deformation theory.

Employing nonlinear thermo elastic version of Love's first approximation theory, the study on the buckling and post buckling response of composite shells subjected to high temperature has been carried out by Birman and Bert [13]. The nonlinear thermal buckling behavior of laminated cylindrical shells in the presence of near the surface del amination has also been studied in [14]. Hosseini Kordkheili et al. [15,16] have employed a particular linearization method to derive the updated Lagrangian finite element formulation for geometrically nonlinear analysis of shell structures. Using their own formulation they succeeded to model snap-through and snap-back buckling phenomena in shell structures with less computational efforts.

The thermo elastic instability problem of conical shells have been investigated in the literature [17–23]. However, in all of these studies, the conical shell is pristine and geometrical defects have not been considered. Patel et al. [24] have analyzed thermal linear buckling and post buckling of laminated cross-ply truncated circular conical shells. They have concluded that for conical shells with small semi cone angle and a length/radius ratio of larger than 1, the linear and nonlinear solution lead to the results with around 5 percent difference.

Sofiyev [25, 26] has considered a sine or cosine function to form axisymmetric geometrical defects during thermal buckling analysis of isotropic conical shell structures. Also, Huang and Han [27] have studied buckling of imperfect FG made cylindrical shells under axial compression.

This paper is motivated to propose a design tool for thermal buckling behavior of truncated thin conical liner reinforced by laminated composite with a general shaped geometric initial defect in liner which is widely observed in the industry. For this purpose, the 8-noded degenerated shell element is employed with various thicknesses in nodes to model thickness variation of composite shell which occurs during the filament winding process. A homemade finite element code is also developed to simply model and apply various boundary conditions as well as various imperfection positions and sizes. In order to show the accuracy and capability of the presented finite element formulation, some examples are solved and the results are compared with those available in the literature.

Finite element modeling of composite fiber reinforced shells

Geometry and kinematics of the shell element

In this study, the 8-noded 3D-shell element of Fig. 1 with five degrees of freedom at each no deisused. This continuum-based degenerated shell element is widely employed in finite element commercial software. Therefore, its implementation into the different practical problems has always been of interest in the literature.

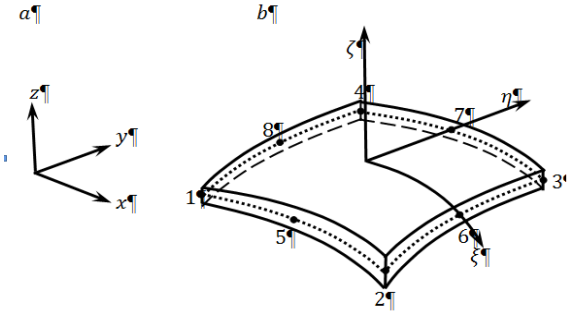

Figure 1.(a) Global coordinate system, (b) The eight-node shell element with natural coordinate system, (c) Unit normal vectors on node iand two rotation local degrees of freedom

For this element geometry is expressed using:

$$\begin{Bmatrix} x \\ y \\ z \end{Bmatrix} = \sum_{i=1}^{8} N_i \begin{Bmatrix} x_i \\ y_i \\ z_i \end{Bmatrix} + \frac{\zeta}{2} \sum_{i=1}^{8} t_i N_i \begin{Bmatrix} V_{nx}^i \\ V_{ny}^i \\ V_{nz}^i \end{Bmatrix} \quad (1)$$

Where V_{nx}^i, V^i_{ny} and V_{nz}^i are local normal vector components, t_i and N_i are respectively thickness and shape function in $\xi\eta$ plane at node i. The first part of these equations expresses the configuration of the shell's middle surface and itsn second part, which contains the unit normal vector, expresses any position between the top and the bottom surfaces of the shell in the thickness direction. In this manner, all terms derived in this study refer to the natural coordinates. The natural coordinates together with the normal vectors of the middle surface represent the geometry of the shell. Each node has five degrees of freedom, three translations in the directions of the global axes, and two rotations with respect to the orthogonal axes normal to thickness direction. The displacement field with in this is isoperimetric shell element which is interpolated as follows:

$$\begin{Bmatrix} u \\ v \\ w \end{Bmatrix} = \sum_{i=1}^{8} N_i(\xi,\eta) \begin{Bmatrix} u_i \\ v_i \\ w_i \end{Bmatrix} + \sum_{i=1}^{8} N_i(\xi,\eta)\zeta \frac{t_i}{2} \begin{bmatrix} -l_{2i} & l_{1i} \\ -m_{2i} & m_{1i} \\ -n_{2i} & n_{1i} \end{bmatrix} \begin{Bmatrix} \alpha_i \\ \beta_i \end{Bmatrix} \quad (2)$$

In order for physical justification, the drilling (sixth) degree of freedom is also adopted during the assembly of the stiffness matrices. Thus, the number of degrees of freedom for each element grows to 48. All the details related to this element for isotropic shells and for composite shells are presented, respectively, in Ref [3,4] and Ref [2].

Finite element formulation for filament winding composite shell structures

During filament winding process around truncated conical shells, since the volume of the fiber across each specific cross-section along the axial direction remains constant, the thickness of each layer at the small end is larger than the large end [29].This statement together with the existence of metallic layer with constant thickness motivated us to develop a finite element formulation for composite material reinforced liner. For this purpose, the multilayered variable thickness element of Fig. 2 is considered.
The finite element formulation for the linear static analysis of the shell structure by considering pre-stresses is as follows:

$$([K]+[K_\sigma])\{q\} = \{F_T\} \quad (3)$$

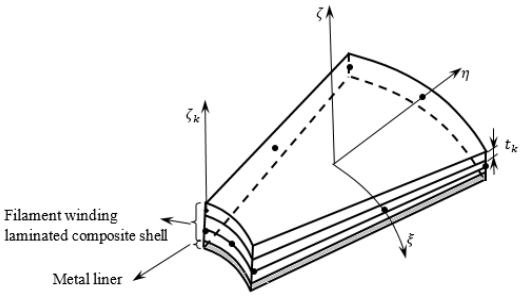

Figure 2. Filament winding variable thickness composite shell element with metal liner

In equation (3), $[K]$ is the stiffness matrix, $[K_\sigma]$ is the geometry matrix, $\{q\}$ is the nodal degrees of freedom vector, and $\{F_T\}$ is the load vector applied on the structure. In natural coordinates, the element stiffness matrix and geo metric matrix are obtained in these forms:

$$[K] = \int [B]^T [D][B]\, dV \quad (4)$$

$$[K_\sigma] = \int [G]^T \begin{bmatrix} [s] & [0] & [0] \\ [0] & [s] & [0] \\ [0] & [0] & [s] \end{bmatrix} [G]\, dV \quad (5)$$

In the above equations, $[G]$, $[B]$ and $[s]$ are respectively the differentiation operator matrix, strain-displacement matrix and Cauchy stress tensor. The load vector $\{F_T\}$ includes the external loadings applied on the shell structure such as the mechanical and thermal loadings. In the natural coordinate system, the element load vector due to the thermal strain is calculated as:

$$\{F_T\} = \int [B]^T \sigma_T\, dV = \Delta T \int [B]^T [D]^k \{\alpha\}^k\, dV \quad (6)$$

In order to avoid the shear locking phenomena, a reduced (2×2×2) order numerical integration scheme is applied for Eqs. (4)–(6) on the volume of the degenerated shell element.

It should be noted that, due to the change in the properties in the thickness (ζ-)direction from one layer to another, this integration for multilayered shell element is not simply similar to single layer shell. In order to deal with this problem, it is necessary to have the integration for each layer separately. So, the thickness coordinate system is modified in such a way that

ζ_k still varies from -1 to +1 for each layer. As the variation range of ζ is between -1 to +1 for the whole shell thickness, the relationship between ζ and ζ_k is defined as below [2]:

$$\zeta = -1 + \frac{1}{t}\left[-t_k(1-\zeta_k) + 2\sum_{l=1}^{j} t_l \right] \quad (7)$$

According to this approach and knowing from (7) that $d\zeta = \frac{t_k}{t} d\zeta_k$, equations (4), (5) and (6) are rewritten in the following forms for multilayered shell element:

$$[K] = \sum_{k=1}^{NL} \int_{-1}^{1}\int_{-1}^{1}\int_{-1}^{1} [B^T][D]_k[B]|J|\frac{t_k}{t} d\xi d\eta d\zeta_k \quad (8)$$

$$\left[K_\sigma\right] = \sum_{k=1}^{NL} \int_{-1}^{1}\int_{-1}^{1}\int_{-1}^{1} [G]^T \begin{bmatrix} [s] & [0] & [0] \\ [0] & [s] & [0] \\ [0] & [0] & [s] \end{bmatrix} [G]|J|\frac{t_k}{t} d\xi d\eta d\zeta_k \quad (9)$$

$$\{F_T\} = \sum_{k=1}^{NL} \Delta T_k \int_{-1}^{1}\int_{-1}^{1}\int_{-1}^{1} [B]^T [D]^k \{\alpha\}^k |J|\frac{t_k}{t} d\xi d\eta d\zeta_k \quad (10)$$

Considering metal liner as one layer with different elastic properties, we can use relations (8) (10) for filament winding variable thickness composite shell element with metal liner Fig. 2.

Eigen buckling solution algorithm

Using linear bucking solution scheme, normally we are able to estimate critical load value and its proportional mode shape for structures. Here, the eigenvalue method together with the iterative solution algorithm of Fig. 3 are adopted to extract the critical load value .Based on this algorithm, the structure is initially imposed to an arbitrary reference level of thermal nodal load, $\{F_T\}_{ref}$, which is linearly proportional to the critical buckling load with as calar multiplier λ_{cr}. Therefore:

$$\{F_T\}_{cr} = \lambda_{cr}\{F_T\}_{ref} \quad (11)$$

Using this arbitrary load vector, a standard linear static analysis is performed to determine the element stresses level. Then, the reference geometric matrix, $[K_\sigma]_{ref}$, is calculated employing these stress values as bellow:

$$[K_\sigma]_{cr} = \lambda_{cr}[K_\sigma]_{ref} \quad (12)$$

Substituting Eqs (11) and (12) into (1) results in:

$$\left([K] + \lambda_{cr}[K_\sigma]_{ref}\right)\{q\}_{ref} = \lambda_{cr}\{F_T\}_{ref} \quad (13)$$

Let the buckling displacements $\{\delta q\}$ relative to reference displacements $\{q\}_{ref}$ vector, load value does not change at the buckling condition. So one can write:

$$\left([K] + \lambda_{cr}[K_\sigma]_{ref}\right)\{q_{ref} + \delta q\} = \lambda_{cr}\{F_T\}_{ref} \quad (14)$$

Now, comparing Eqs (13) and (14) yields:

$$\left([K] + \lambda_{cr}[K_\sigma]_{ref}\right)\{\delta q\} = 0 \quad (15)$$

Equation (15) is the eigenvalue buckling equation. The solution of this equation estimates smallest positive eigenvalue and its eigenvector. In next iteration, the structure is loaded by $\lambda_{cr}\{F_T\}_{ref}$ and the algorithm is repeated until the difference between eigenvalue in two sequential steps is less than 0.01 [3], this eigenvalue and its proportional eigenvector are critical buckling load and mode shape, respectively.

Numerical examples

Using the finite element formulation of the filament winding composite shell element discussed in this paper, an in-house finite element program has been developed. Some available problems in the literature are performed and the results are compared for verifying the present formulation and showing its capabilities.

The derived finite element formulation of the shell element together with the proposed Eigen buckling analysis algorithm have been applied in a finite element program. Using this program, some sample problems are solved to show the performance of the present finite element shell formulation. The material properties used in this work, are presented in Table 1. These properties are written in 27°C.

Table 1. The material properties in this study

SUS304	
$\boldsymbol{E(Gpa)}$	207.7
$\boldsymbol{\nu}$	0.3177
$\boldsymbol{\alpha(1/°C)}$	1.52e-5
$\boldsymbol{\rho(Kg/m^3)}$	8166
Laminated composite	
$\boldsymbol{E_L(Gpa)}$	172.55
$\boldsymbol{E_T(Gpa)}$	6.89
$\boldsymbol{\nu_{LT}, \nu_{TT}}$	0.25
$\boldsymbol{G_{LT}(Gpa)}$	3.445
$\boldsymbol{G_{TT}(Gpa)}$	1.378
$\boldsymbol{\alpha_L(1/°C)}$	6.3e-6
$\boldsymbol{\alpha_T(1/°C)}$	1.89e-5
$\boldsymbol{\rho(Kg/m^3)}$	1560

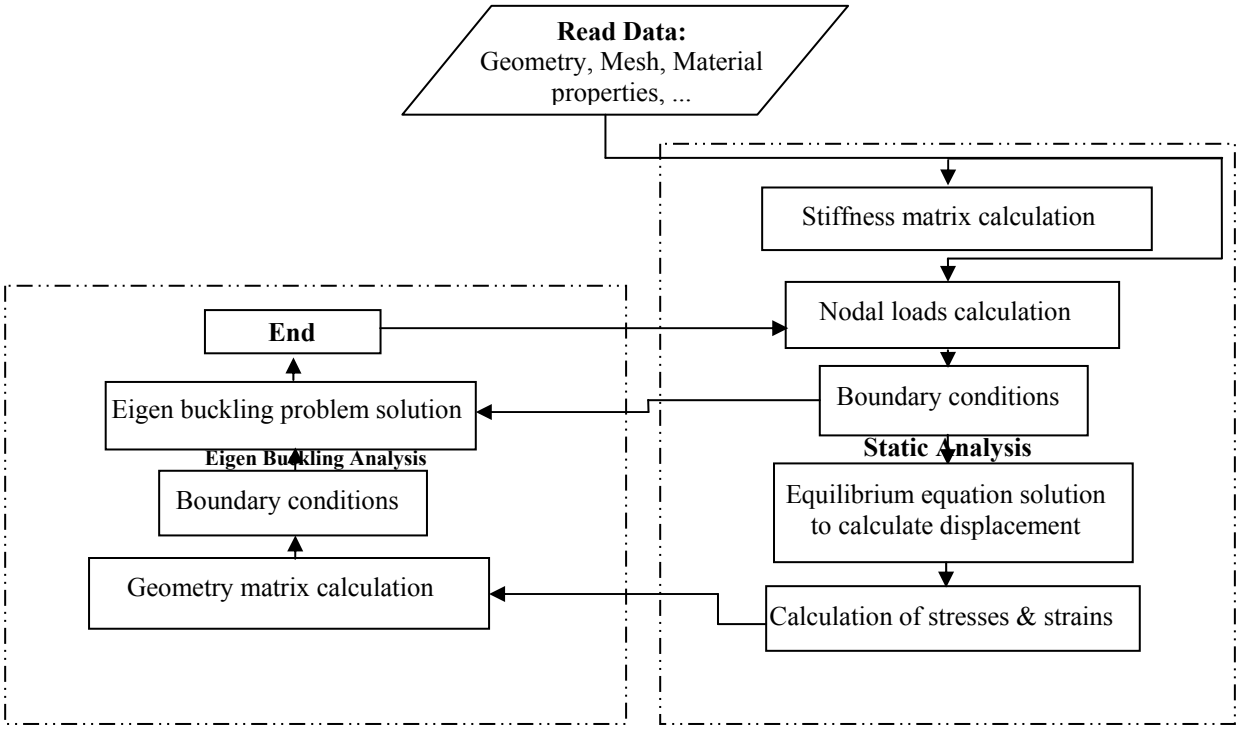

Figure 3. Eigen buckling analysis algorithm flowchart

Convergence study

In order to determine the finite element mesh size and suitable number of elements, a convergence study is initially carried out to represent the correct buckling load and mode shape in truncated conical shells. For this purpose, the isotropic truncated conical shell of Fig. 4 made of SUS304 with $\frac{l}{r} = 1.0438$and$\frac{r}{t} = 100$, and having a mean radius equal to 0.876 m is considered.

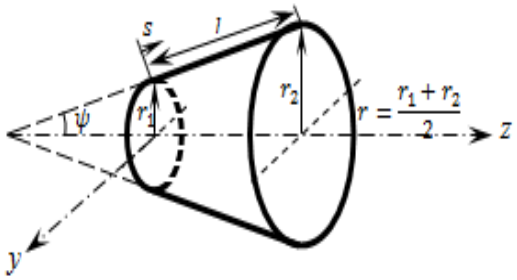

Figure 4. Geometry of problem

Bhangale et al [6] employed axisymmetric linear finite element formulation to solve this problem for FG conical shells. For semi-vertex angle ψ=0°,they reported thermal buckling results for a cylinder made ofSUS304. Therefore, the same problem is chosen here in order to ensure the accuracy of the proposed finite element model. Results from the present work and those from Ref. [6] are compared in Table 2.

Table 2. Convergence study of critical temperature (°C)

	Present work				Bhangale et al. [6]
	Number of elements				
	252	640	1072	2720	
	Normalized size of element($element\ size/r$)				
	0.1769	0.1141	0.0856	0.0580	
Critical temperature	688.33	620.12	605.35	604.29	598.98

It can be observed that for element size of average radius ratio around 0.08, theconvergence is achieved and the results are also comparable with those in Ref [6]. This size of elements are also employed to solve all other problems.

Verification of the finite element formulation

With regard to the lack of available data for thermal buckling of liner-composite shell due to the imperfection in the literature, the validation process is carried out in three conditions: (1) the critical buckling temperature of laminated composite truncated conical shells without imperfection, (2) the critical buckling temperature of laminated composite cylindrical shells with axisymmetric imperfection, and (3) the critical buckling temperature of isotropic cylindrical shells with local wavy imperfection.

Conical composite shell without imperfection

In this example, conical cross-ply composite shells with r/t=100 and l/r=1 are investigated. Here, dependency of material properties on temperature is not considered and temperature distribution is assumed uniform in the thickness direction. Patel et al. [24] have carried out a finite element deflection analysis based on first-order shear deformation theory to solve this problem. The critical temperature parameter $\Delta T \alpha_L \frac{r_1}{t}$ is employed to report and compare the results, where α_L is the longitudinal coefficient of expansion. Fig. 5 compares the results from the present work and those from linear and nonlinear solutions in Ref [24] for both C-C and S-S boundary conditions. In these figures, one can observe that there are very good agreements between the results from the present work formulation and those from linear solution [24]. Also it can be seen that the difference between linear and nonlinear solutions is dependent on boundary conditions as well as the semi cone angle. However, for all cases nonlinear solution predicts a higher critical temperature parameter while linear solution will lead to a more conservative design.

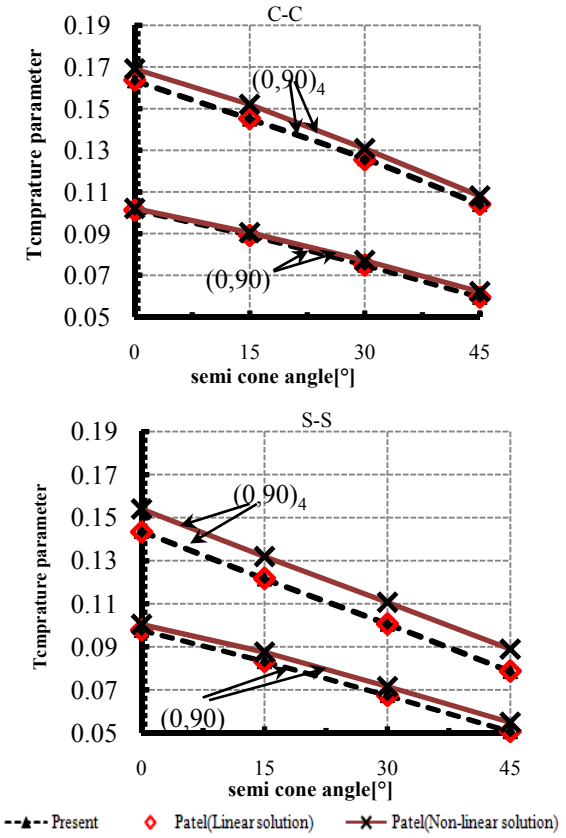

Figure 5. Verification of critical temperature parameters with boundary conditions C-C, S-S and comparison between linear and nonlinear solutions

Cylindrical composite shell with axisymmetric imperfection

Huang and Han [27] have employed Donnell theory to study buckling of FG cylindrical shells with axisymmetric imperfection imposed by axial compression loading. They defined imperfection using $w_0 = \mu t \sin\left(\frac{n\pi s}{L}\right)$, where μ is the magnitude coefficient of the geometric imperfection. They also reported the results for Ti6Al4V made cylinder with temperature-dependent properties at 300K.The same problem has been solved here using both present formulation and ANSYS commercial software. According to the results listed in Table 3,it can be observed that the present solutions are consistent with those of ANSYS. Also, there is a discrepancy of less than 2% between the present solutions and those reported in Ref. [27]. Moreover, it can be observed that increasing the number of waves in axisymmetric imperfection causes a decrease in the critical compressive stress.

Table 3. Imperfection affection the critical compressive stress (Mpa) in S-S cylindrical shell (T_0=300 K, ΔT=0, l/r=2, r/t=200)

Imp. Magnitude	Ref [27]	Present	ANSYS 14.0
$\boldsymbol{\mu = 0}$	300.48	304.48	304.22
$\boldsymbol{\mu = 0.5, n = 1}$	273.73	268.23	268.94
$\boldsymbol{\mu = 0.5, n = 3}$	221.45	218.28	219.03

Cylindrical isotropic shell with local wavy imperfection

In this study, a clamped supported cylindrical shell with local wavy imperfection under external pressure has been investigated. All of the geometrical parameters of local imperfection are shown in Fig.6.In this picture, radius of imperfection is obtained by equation $\tilde{r}(\theta, z) = r - \left(1 + \cos\left(\frac{2\pi\theta}{\theta_0}\right)\right)\left(1 + \cos\left(\frac{\pi z}{a}\right)\right)$. This problem is chosen from Khaled [28] work and the same materials, A36 and Grade 80 steel, are studied here as reported in [28]. Khaled [28] has employed finite element commercial software of ANSYS to solve this problem. Also, a normalized critical pressure is obtained by $P(1-\nu^2)/E$.

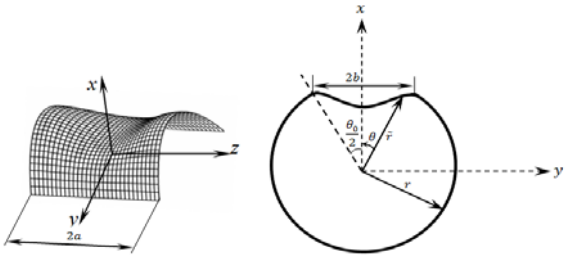

Figure 6. Geometrical parameters of local imperfection

The results of this investigation are collected in Table 4. The present solutions compared with the finite element solution [28] as well as a good agreement between the results are observed.

Table 4. C-C cylindrical shell with local wavy imperfection

Material			A36		Grade 80	
			$P(1-\nu^2)/(E(t/D)^{2.2})$		$P(1-\nu^2)/(E(t/D)^{2.2})$	
$l/2r$	a/b	t/r	Present	Ref. [28]	Present	Ref. [28]
4	2	0.01	0.3011	0.2910	0.5215	0.5010
4	5	0.01	0.3647	0.3500	0.5870	0.5628
10	2	0.01	0.2701	0.2633	0.4637	0.4489
10	5	0.01	0.3010	0.2928	0.5055	0.4903
10	2	0.02	0.2723	0.2644	0.4529	0.4398
10	5	0.02	0.2450	0.2388	0.4051	0.3936

In order to show the capabilities of the presented formulation as a design tool for analysis of liner-reinforced composite truncated conical shell structures in the presence of asymmetric imperfection, some examples are solved in this section. The results are discussed and general conclusions are reported.

Effects of local imperfections on thermal buckling behavior of conical liner only

To show the effects of local imperfection size and position on thermal bucking behavior of conical liner only, 36 cases of asymmetric imperfection are studied in this section. The shell made by SUS304 material of Table 1, $r_1/t = 100$, $l/r_1 = 1$ and $\psi = 15$areconsidered with imperfection geometries in Table 5.

The results of this studyfor boundary conditions C-C, S-S and C-Fare shown in Fig. 7. The critical temperature parameter $\Delta T\alpha_{liner}\frac{r_1}{t}$is employed to report and compare the results.

Table 5. Geometric properties of imperfections

Imperfection geometry	Type	*a*	*b*
Linear curve Circular curve 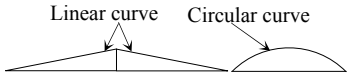 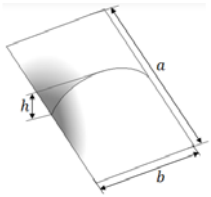 *Imperfection geometry when located in the middle of the shell*	I	$\frac{3l}{8}\cos(\psi)$	$2r_1\sin(10°)$
Linear curve Circular curve 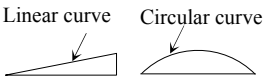 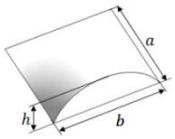 *Imperfection geometry when located in the ends of the shell*	II	$\frac{2l}{8}\cos(\psi)$	$2r_1\sin(6.65°)$
	III	$\frac{l}{8}\cos(\psi)$	$2r_1\sin(3.32°)$

The case studies

From these figures some important points can be noted as follows:

- For all cases of study, as it could be predicted, for *h/t*=0 the corresponding critical temperatures are the same for the same boundary conditions.
- For the C-C boundary conditions, the greatest decrease in critical temperature parameter occurs when the defect exists in the middle section of the truncated conical shell.
- In contradictory with the previous point, for S-S boundary conditions, imperfections at the edges of the cone cause a greater decrease in critical temperature parameter, since rotations are allowed over the two edges.
- For C-F boundary conditions(with clamped small end)the free edgeallows the structure to

expand. Therefore, in this case the critical temperature parameter rises rapidly. On the other hand, there is no buckling in operational temperature of the liner with $l/r_1 = 1$.

- In the C-C boundary conditions, the defects in the form of bumps are more effective in reducing the critical temperature parameter rather than defects in the form of lobs. UnderS-S boundary conditions, in most of the cases, bumps cause greater decrease at the critical temperature parameter.

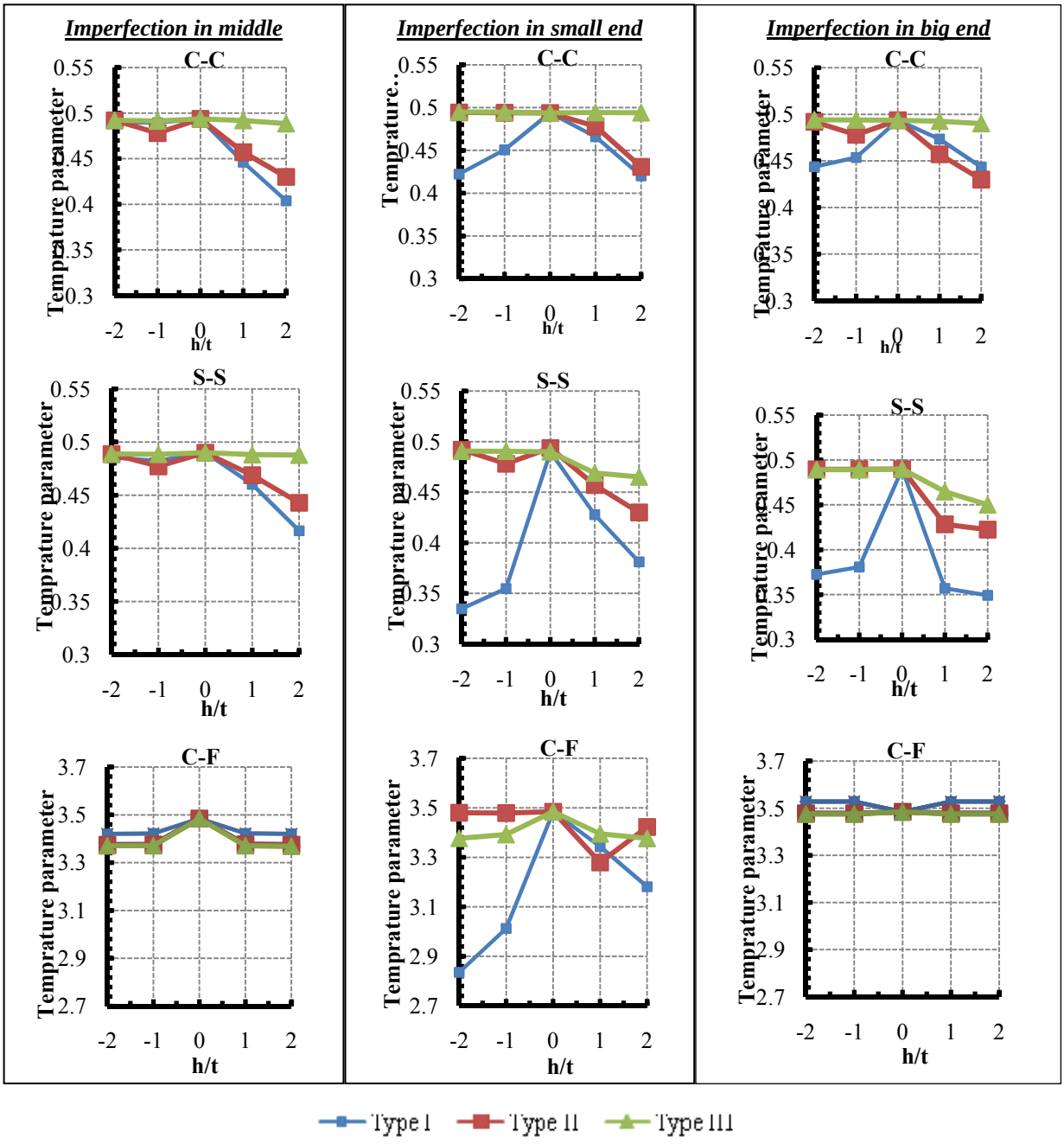

Figure 7. Temperature parameter versus *h/t* ratio for different boundary conditions as well as different types of imperfection in liner only

Effect of increase in reinforced composite shell thickness on thermal buckling behavior of conical liner

In this problem, the same truncated conical liner with reinforced composite shell $[-45, 45, 45,-45]_s$ is analyzed with boundary conditions S-S only and the middle imperfection Type I. Four different cases $\frac{t_{comp}}{t_{liner}} = 0, \frac{1}{8}, \frac{1}{4}, \frac{1}{2}$ are considered in this study where t_{comp} and t_{liner} are the reinforcement composite shell and the conical liner thicknesses, respectively. The results of this investigation are depicted in Figs.8 and 9.In Fig. 8, the sketched straight line shows the critical buckling temperature for the case of liner only without imperfection. From these figures, it can be inferred that the increase int_{comp} with respect tot_{liner} resultsin an increase in the critical buckling temperature, as could be expected. While for $\frac{h}{t} \leq 2$, $\frac{t_{comp}}{t_{liner}} = \frac{1}{8}$. Although the defected liner has been reinforced, it is not enough to eliminate the imperfection effects. But for $\frac{t_{comp}}{t_{liner}} = \frac{1}{4}$, the defected liner has been reinforced enough and the the effects of imperfection no longer exist. Finally, for the $\frac{t_{comp}}{t_{liner}} = \frac{1}{2}$, there is no buckling in operational temperature range of the liner with a suitable margin of safety.

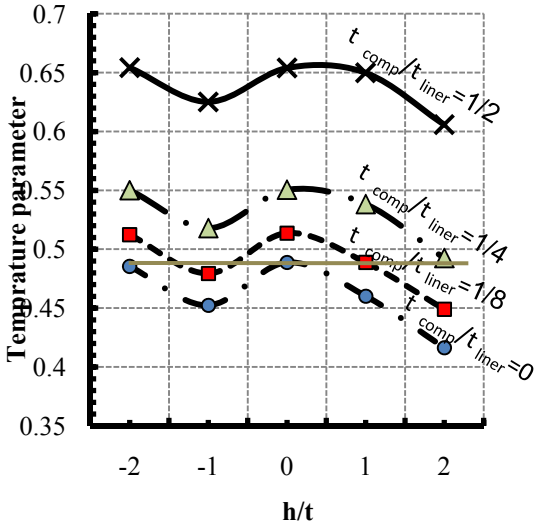

Figure 8. Effects of the increase of reinforced composite shell thickness, S-S

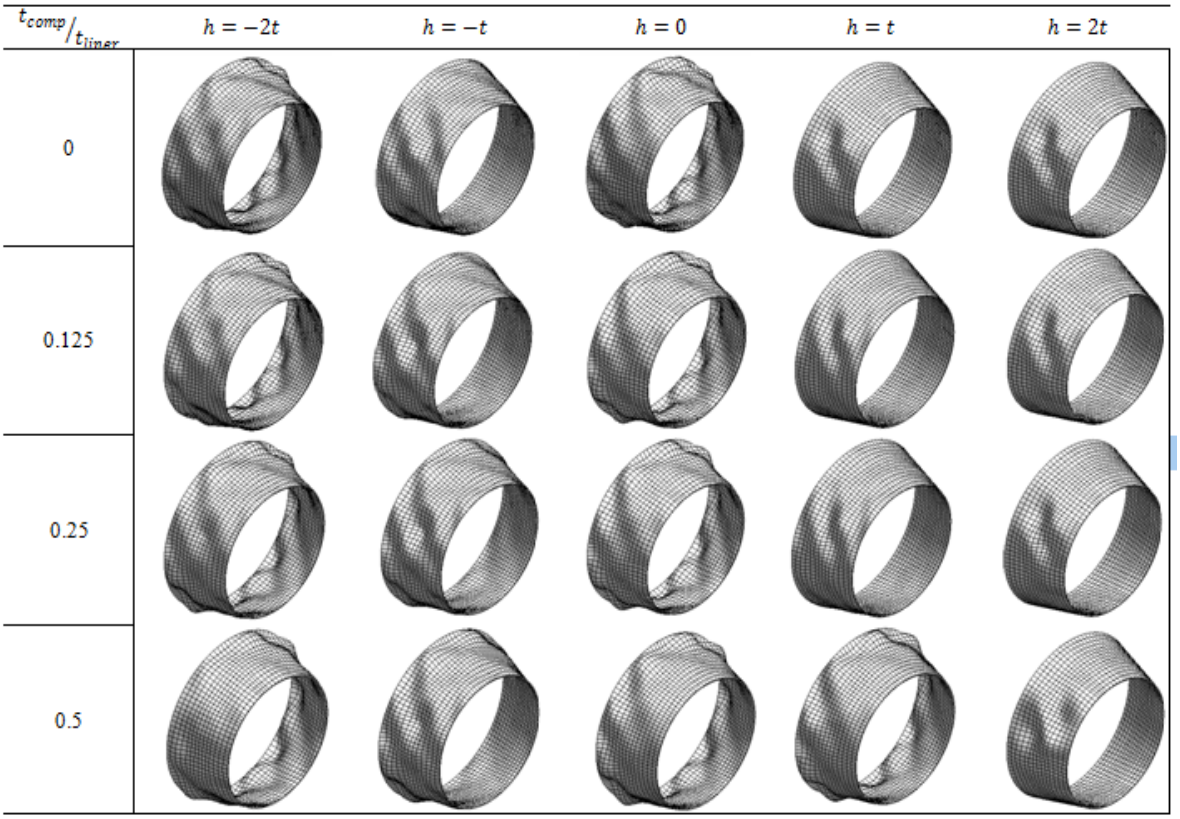

Figure 9. Buckling modes corresponding to critical buckling, S-S, related to Fig.8

Variation of thickness effects on thermal buckling behavior of filament winding truncated conical shell with liner

As it was mentioned previously, during filament winding process, the thickness of each layer at the small end is greater than that at the large end. The variable thickness can be estimated using:

$$t_k = t_{1k}\left(\frac{r_1}{r_1 + z\tan(\psi)}\right) \qquad (16)$$

where t_{1k} is the thickness of the layer at the small end. In this section, the same reinforced conical liner with composite arrangement [-45, 45, 45,-45]s, $\frac{l}{r_1} = 1$ and $\psi = 15°$is considered. For the case of restriction on total thickness of conical shell, two possible cases $\frac{t_{2-comp}}{t_{liner}} = \frac{1}{2}$, $\frac{r_1}{t_2} = 100$ (i. e. C1 case) and $\frac{t_{1-comp}}{t_{liner}} = \frac{1}{2}\frac{r_1}{t_1} = 100$ (i. e. C2 case) as shown in Fig. 10 are considered in this study, where t_{1-comp} and$t_{2-comp}$are reinforced composite thickness at small and large ends, respectively. As shown in this figure, in both cases composite thickness in the small end is greater than that at the large end. But in the case ofC1, change in the thickness starts from the restricted value and increases toward the small end. However, in C2 case, the thickness variation is starts from a smaller value and approaches to a restricted one toward the small end. Therefore, having limitation on maximum thickness of conical shell may largely affect the reinforcement layers geometry and thickness during filament winding process.

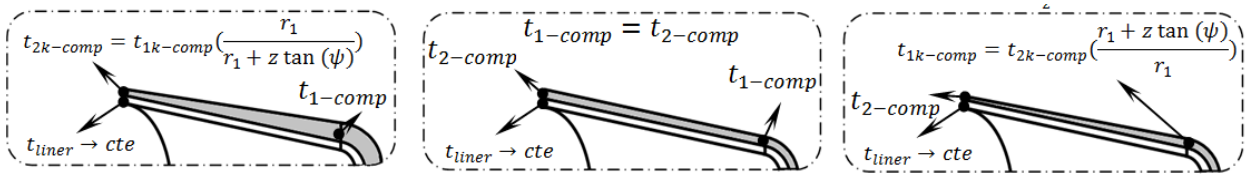

C1 case *C2* case

Figure 10. The case study of total thickness of conical shell

In this section, the results are presented and compared for both with and without considering variable thickness of reinforced composite shell. In all cases, liner thickness is assumed to be constant. Considering different boundary conditions for conical shells, critical temperature versus h/t_2 as well as critical mode shapes are depicted in Figs. 11 - 14.

Here, we are interested in considering this limitation effect on critical temperature of the conical shell. For this purpose, the worst imperfection cases for C-C and S-S boundary condition obtained from the previous sections are considered.

The imperfection of types *I* and *II* are taken to be placed in the middle section of the liner for C-C boundary condition. Regarding Fig. 11,applying thickness variation due to filament winding process may have significant effects on critical temperature value in the presence of imperfections type I and II. Additionally, it is observed that applying correct restriction on reinforced thickness is vital during truncated conical shell analysis. For example, if we use constant composite shell thickness to analyze the structure instead of practical cases *C*1 and*C2,* our final structure will be overweight or unsafe, respectively. Also it is noted that the imperfection size and types effects are totally nonlinear, hence, preparing a design tool like the one we proposed in this work is always needed during truncated reinforced conical shell design and production. Also imprecation may cause deformation of the liner configuration from axisymmetric configuration and this may affect the performance of the structure. From Fig. 12,one can observe that buckling waves are greatly affected by imperfection types. Also as it can be predicted, local waves are dense around the big end.

Type *I* imperfection as the worst case is considered here for boundary conditions S-S, and imperfection has been taken place in small/big ends. The results are plotted in Figs. 13 and 14. According to Fig. 13, for the case with imperfection in small end, applying limitation C1 causes higher critical temperature parameter, while we do not see the effects of imperfection further. Moreover, from this figure and comparing the critical temperature variation for case C2 with case t=cte, it is observed that a general statement cannot

be achieved for this case. The reason is that for h/t1 from -2 up to -1, critical temperature increases in comparison with case t=cte and after this however for case t=cte we have a rapid change in critical temperature parameter up to h/t=0.Then it rapidly decreases, but for case C2 changes happened smoothly. For the conical shell with S-S boundary condition and imperfection at big end, the behavior has approximately the same trend for all cases. However, ignoring model thickness variation with correct thickness restriction leads to an inaccurate design

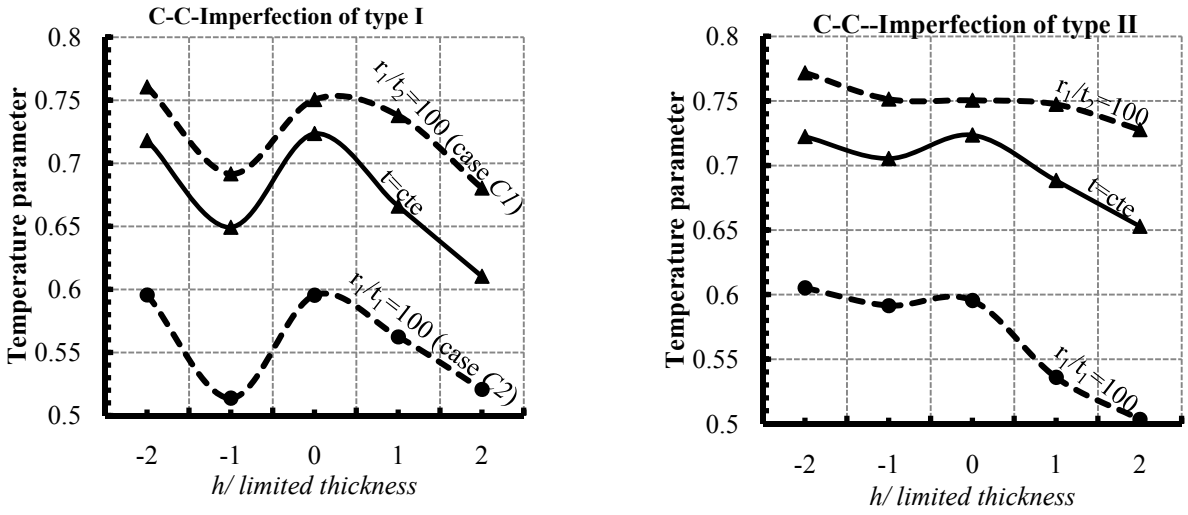

Figure 11. Effects of variable/constant reinforced composite shell thickness and effects of geometrical parameters of imperfection with boundary conditions C-C.

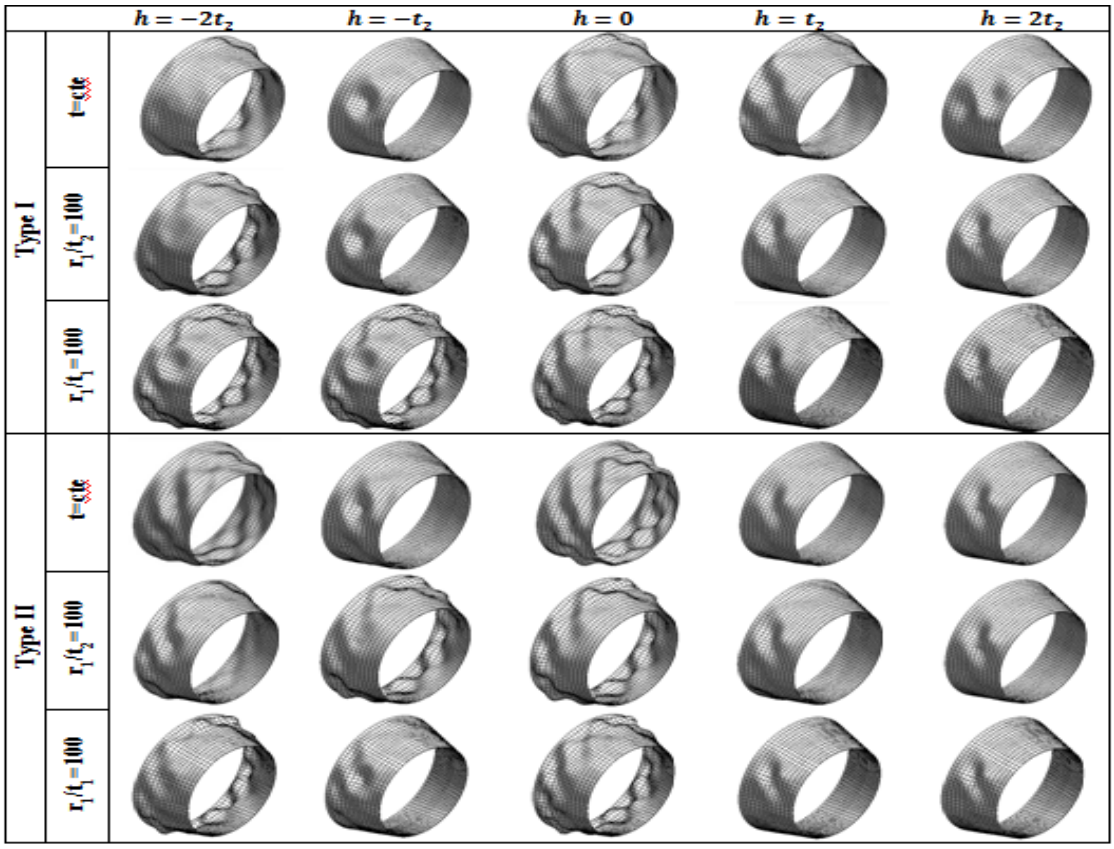

Figure 12. Buckling modes corresponding to critical buckling temperatures in Fig. 11

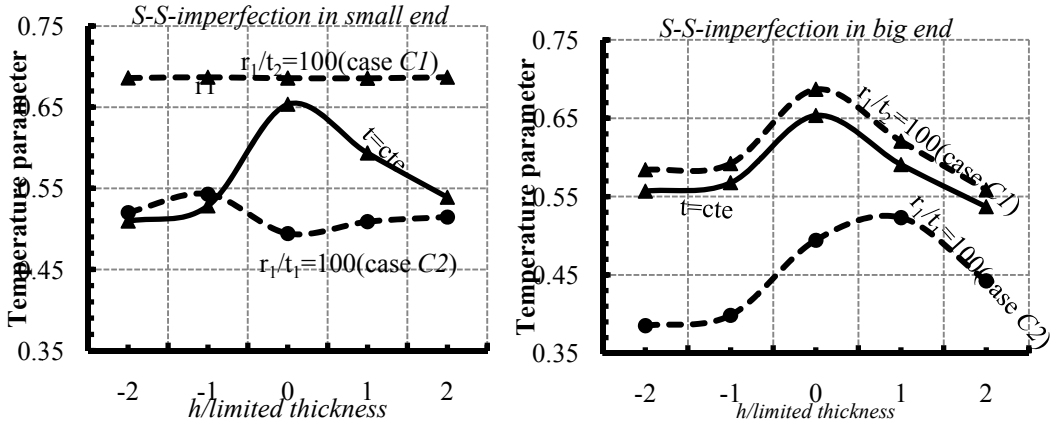

Figure 13.Effects of variable/constant reinforced composite shell thickness and effects of imperfection size and position with boundary conditions S-S

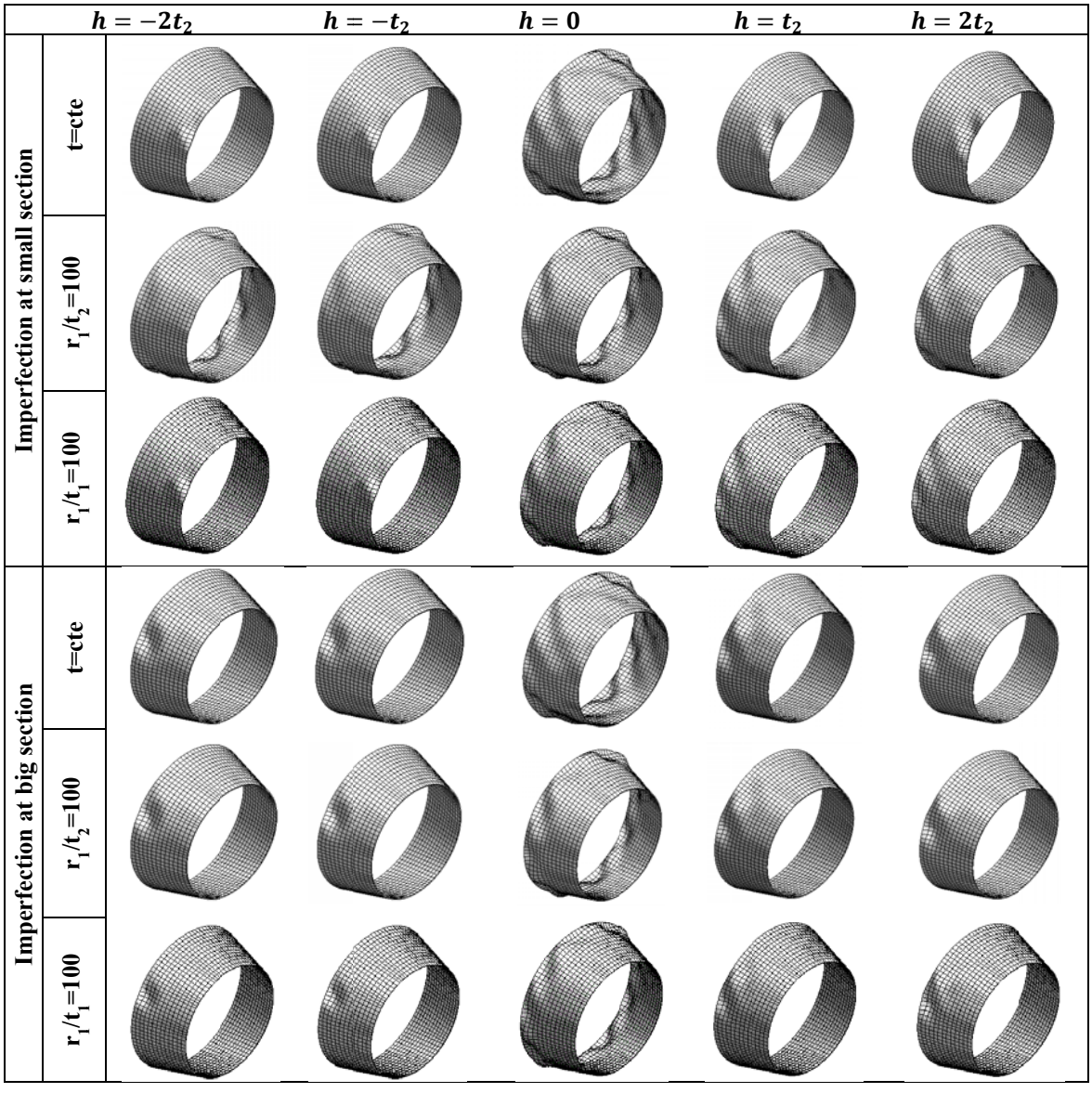

Figure. 14. Buckling modes corresponding to critical buckling temperatures in Fig.13

Fig. 14 illustrated that in cases C1 and C2 although the small end includes imperfections, the wave buckling appears at the large end when the variable thickness is taken into account during analysis. It means that filament winding process not only increases the thermal buckling of the truncated shell, but also may eliminate some imperfection effects that may occur during production course. This is a case dependent statement and should be studied case by case.

Conclusions

In this paper, local imperfection size and position effects on thermal buckling behavior of composite fiber reinforced truncated conical liner were investigated. The conical shells were analyzed with three types of boundary conditions c-c, s-s and c-f. In the first step, the conical liners with SUS304 material and with 36 types of imperfections were analyzed. Then, the most critical sizes and positions of imperfections were recognized at each type of boundary conditions. Next, effect of reinforced laminated composite shell thickness on critical buckling temperature was studied and a suitable thickness was selected. In the final step, thermal buckling behavior was studied for the most critical sizes and positions of imperfection at each of the boundary conditions along with considering the liner constant thickness and reinforced composite shell constant/variable thickness.

According to the results, there is no general statement for effects of imperfection on thermal buckling behavior of filament winding reinforced truncated conical shell structures. Therefore, analysis is necessary for each case. The presented finite element solution provides designers with a suitable tool to quickly investigate nonlinear imperfection effects that are normally associated with metallic linear during their production after CMM to make sure their critical buckling temperature after filament winding process.

References

[1] L., Vibration of Shells, Washington D.C.: National Aeronautics and Space Administration, 1973.

[2] S. Panda and R. Natarajan, "Analysis of Laminated Composite Shell Structures by Finite Element Method," Composite Structures, Vol. 14, 1981, pp. 225-230.

[3] R.D. Cook and R.D. Witt, Concepts and Applications of Finite Element Analysis, Wiley, Fourth Ed., Wisconsin- Medison: CRC Press, part 5, pp: 650-667, 2001.

[4] Klaus and J. Bathe, *Finite Element Procedures*, McGraw-Hill Pablished, Fourtheen Ed., BocaRaton, Fl, USA: CRC Press, part 5, pp: 400-503, 1967.

[5] R. Naj, M. Sabzikar Boroujerdy, and M. Eslami, "Thermal and Mechanical Instability of Functionally Graded Truncated Conical Shells," *Thin-Walled Structures*, Vol.46, 2008, pp.65-78.

[6] R. Bhangale, N. Ganesan, and C. Padmanabhan, "Linear Thermo Elastic Buckling and Free Vibration Behavior of Functionally Graded Truncated Conical Shells," *Journal of Sound and Vibration*, Vol. 292, 2006, pp. 341-371.

[7] Gupta, S.D., Wang I-C. Thermal Buckling of Orthotropic Cylindrical Shells. Fiber Sci Technol, Vol. 6, 1973, pp. 39–45.

[8] S. K. Radhamohan and J. Venkatramana, "Thermal buckling of orthotropic cylindrical shells," *J AIAA* Vol. 13, No. 3, 1975, pp. 397–399.

[9] R.K., Thangartnam, R, Palaninathan and J. Ramachandran, "Buckling of composite cylindrical shells," *J Aero SocIndia*, Vol. 41, No. 1, 1989, pp. 47–54.

[10] R.K., Thangartnam, R, Palaninathan and J. Ramachandran, "Thermal buckling of laminated composite shells," *J AIAA*, Vol. 28, No. 5, 1990, pp. 859–60.

[11] Ganesan N, Kadoli R. "Buckling and dynamic analysis of piezo thermo elastic composite cylindrical shells," *Compos Struct*, Vol. 59, No. 1, 2003, pp. 45–60.

[12] Kadoli R, Ganesan N., "Free vibration and buckling analysis of composite cylindrical shells conveying hot fluid," *Compos Struct*, Vol. 60, 2003, pp.19–32.

[13] Birman V, Bert CW. "Buckling and post-buckling of composite plates and shells subjected to elevated temperature," *ASME J Appl Mech*, Vol. 60: 1993, pp. 514–9.

[14] Wang X, Lu G, Xiao DG. "Non-linear thermal buckling for local delamination near the surface of laminated cylindrical shell," *Int J MechSci*,Vol. 44, 2002, pp. 947–65.

[15] S.A. HosseiniKordkheili, R. Naghdabadi, "Geometrically non-linear thermo elastic analysis of functionally graded shells using finite element method," *Int. J. Numer. Meth. Engng*, Vol. 72, 2007, pp. 964–986

[16] S.A. Hosseini Kordkheili, R. Naghdabadi, M. Jabbarzadeh, "A geometrically nonlinear finite element formulation for shells using a particular linearization method," *Finite Elements in Analysis and Design*, Vol. 44 2008, pp.123 – 130.

[17] Bendavid D, Singer J. "Buckling of conical shells heated along a generator," *AIAA J*, Vol. 5, No. 9, 1967, pp. 1710–1713.

[18] Lu SY, Chang LK. "Thermal buckling of conical shells," *AIAA J*, Vol. 5, No. 101967. Pp. 1877–82.

[19] LK, Chang and SY. Lu, "Nonlinear thermal elastic buckling of conical shells," *Nucl Eng*, 1968, Vol. 7, 1978, pp. 159–69.

[20] Tani J., "Influence of axisymmetric initial deflections on the thermal buckling of truncated conical shells," *Nucl Eng*, Vol. 48, 1978, pp. 393–403.

[21] J. Tani, "Buckling of truncated conical shells under combined pressure and heating," *J Therm Stresses*, Vol. 7, 1984, pp. 307–16.

[22] Wu C-P, Chiu S-J. Thermo elastic buckling of laminated composite conical shells. *J Therm Stresses,* Vol. 24, 2001, pp. 881–901.

[23] Wu C-P, Chiu S-J., "Thermally induced dynamic instability of laminated composite conical shells," *J Solids Struct*, Vol. 39, 2002, pp. 3001–21.

[24] B.P. Patel, K.K. Shukla, Y. Nath. "Thermal post buckling analysis of laminated cross-ply truncated circular conical shells," *Composite Structures*, Vol. 71, 2005, pp.101–114

[25] A.H. Sofiyev, "The Stability of Functionally Graded Truncated Conical Shells Subjected to Aperiodic Impulsive Loading," *International Journal of Solids and Structures*, Vol. 41, 2004, pp. 3411-3424.

[26] A.H. Sofiyev and M. Avcar, "The Stability of Cylindrical Shells Containing an FGM Layer Subjected to Axial Load on the Pasternak Foundation," *Scientific Research*, Vol. 2010, 2010, pp. 228-236.

[27] H. Huang, Q. Han. Buckling of imperfect functionally graded cylindrical shells under axial compression. European," *Journal of Mechanics A/Solids*, Vol. 27, 2008, pp. 1026–1036.

[28] Khaled M. El-Sawy. Inelastic stability of liners of cylindrical conduits with local imperfection under external pressure, *Tunnelling and Underground Space Technology* ,Vol. 33, 2013, pp. 98–110

[29] Y. Goldfeld, J. Arbocz, Alan Roth well. "Design and optimization of laminated conical shells for buckling. Thin-Walled Structures," Vol. 43, 2005, pp.107–13.